
Three-frame Algorithm of Car Path Reconstruction from Airborne Traffic Data

Ihor Lubashevsky¹, Namik Gusein-zade¹, Dmitry Klochkov¹, and
Sergey Zuev²

¹ A.M. Prokhorov General Physics Institute, Russian Academy of Sciences,
Vavilov str. 38, Moscow, 119991, Russia, e-mail (IL): ialub@fpl.gpi.ru

² German Aerospace Center, Optimal Information Systems, Rutherfordstrasse 2,
D-12489 Berlin, Germany

Summary. The airborne traffic monitoring system forms a novel technology of detecting vehicle motion. An optical digital camera located on an airborne platform produces a series of images which then are processed to recognize the fixed vehicles. In this way the video data are converted into the time sequence of frames containing the vehicle coordinates. In the present work a three-frame algorithm is developed to identify the succeeding vehicle positions. It is based on finding the neighboring points in the frame sequence characterized by minimal acceleration. To verify and optimize the developed algorithm a “Virtual Road” simulator was created. Finally available empirical data are analyzed using the created algorithm.

Introduction

The traditional techniques of traffic flow measurements are based on local detectors mounted at fixed places of a road network. Such detectors provide adequate information about traffic flow only for road fragments of a rather simple structure. However in cities there are a large number of complex road intersections, where vehicles moving on different branches interact strongly with one another. To measure appropriately traffic flow features on such “hot areas” the information supplied by the stationary detectors should be complemented at least with the detailed information about the spatial structure of traffic streams on these hot areas. Currently the novel technology of airborne monitoring and detecting the main characteristics of traffic flow is under development. The German Aerospace Center (DLR) with its department of Transportation Studies and department of Optical Information Systems has developed an airborne traffic monitoring system which was successfully used during the Soccer World Championship 2007 in Germany [1, 2, 3]. In particular, these and some other DLR airborne datasets are used in the present paper. This system is based on an optical sensor placed on an airborne platform. The optical sensor produces a series of images of area under. The empirical airborne traffic data obtained by recognizing these images form a set of the frames with individual vehicle coordinates. To use these data and to calculate the main parameters of traffic flow trajectories of individual vehicle motion have to be reconstructed. In this way

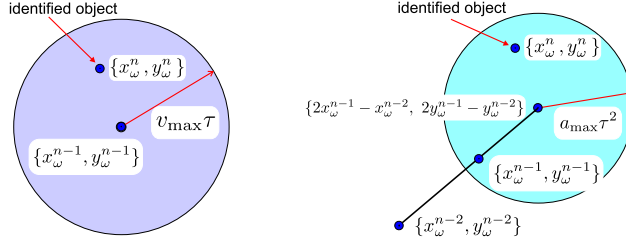


Fig. 1. Illustration of the car identification algorithms. Within the two-frame speed limitation algorithm (left fragment) new objects $\{x^n, y^n\}$ are sought in the circle of radius $r = v_{\max}\tau$ centered at the point $\{x_{\omega}^{n-1}, y_{\omega}^{n-1}\}$. In the three-frame algorithm bounding acceleration (right fragment) new objects $\{x^n, y^n\}$ are sought in the circle of radius $r = a_{\max}\tau^2$ centered at the point $\{2x_{\omega}^{n-1} - x_{\omega}^{n-2}, 2y_{\omega}^{n-1} - y_{\omega}^{n-2}\}$.

it becomes possible to measure the traffic flow rate, the mean velocity of vehicles, and their density simultaneously.

Vehicle Trajectory Reconstruction

The airborne traffic data under consideration are the time series \mathcal{F} of frames $\{F_t\}$ with the coordinates of recognized vehicles, $\mathcal{F} = \{F_t = \{x_\alpha, y_\alpha\}\}$. The problem is to construct a collection of trajectories $\mathcal{P} = \{x(t), y(t)\}_t$ passing through the points $\{\{x_\alpha, y_\alpha\}\}$ at the corresponding time moments $\{t = n\tau\}$, where n is integer and τ is the time span between successive frames. Some constraints should be imposed on the vehicle trajectories \mathcal{P} to make them smooth. There are several ways to do this, in particular, to bound the “acceleration” (the used approach)

$$\sqrt{\left(\frac{d^2x_\alpha}{dt^2}\right)^2 + \left(\frac{d^2y_\alpha}{dt^2}\right)^2} \leq a_{\max} \quad (1a)$$

or to bound the “velocity”

$$\sqrt{\left(\frac{dx_\alpha}{dt}\right)^2 + \left(\frac{dy_\alpha}{dt}\right)^2} \leq v_{\max}. \quad (1b)$$

We note that the acceleration and velocity thresholds, a_{\max} and v_{\max} , are not the real characteristics of car motion but internal algorithm parameters whose choice is determined by its efficiency being highest.

To explain the crux of the algorithm implementing these constraints let us assume that the preceding frames $\{\dots, F_{n-2}, F_{n-1}\}$ have been analyzed and the vehicle trajectories are reconstructed at the previous time moments $\{\dots, n-2, n-1\}$. Then a car $\{x_\alpha^n, y_\alpha^n\}$ in the frame F_n will be incorporated into the trajectory $\omega = \cup_m \{x_\omega^m, y_\omega^m\}$ if

$$\sqrt{(x_\omega^{n-2} - 2x_\omega^{n-1} + x_\alpha^n)^2 + (y_\omega^{n-2} - 2y_\omega^{n-1} + y_\alpha^n)^2} \leq a_{\max} \tau^2. \quad (2)$$

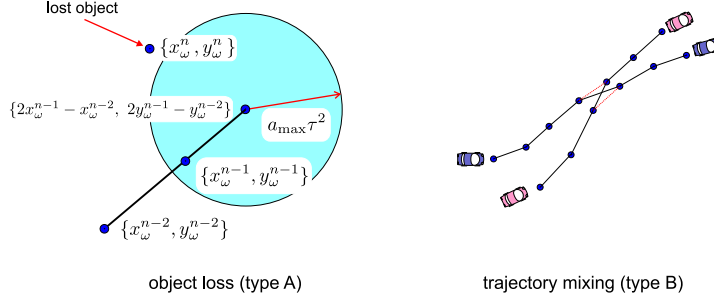


Fig. 2. The main errors of the car identification algorithm.

Figure 1 illustrates the given three-frame algorithm based on (1a) as well as the relative two-frame algorithm based on (1b) mentioned for comparison only.

Let us discuss the possible errors of the car identification algorithm caused by errors in the car coordinate measurements. There are two main types of the latter ones; the errors of individual vehicle positions, ξ_1 , and the errors in the frame reference to GPS, ξ_2 . According to the pilot airborne monitoring system (Institute for Traffic Research, DLR, Berlin) [1, 2] the error values can be estimated as $\xi_1 \sim 0.5$ m and $\xi_2 \sim 1-2$ m. The caused errors of the car identification algorithm, i.e. the object loss (type A) and the trajectory mixing (type B) illustrated in Fig. 2 will be quantified in units of

$$A(B) = \frac{\text{The number of lost(mixed) objects}}{\text{Total number of objects}} \cdot 100\%$$

To analyze the feasibilities of the identification algorithm, first, the following kinematic simulator has been used (Fig. 3, upper fragment). The motion of cars is specified by the shown equations where the parameters x_{0i} , y_{0i} , b_{xi} etc. are random and some addition constraints are imposed to prevent the collisions. The noise components $\xi_{x(y)i} = (\xi_1 + \xi_2)_{x(y)i}$ imitate the errors in the measurements of the car coordinates x_i and y_i at the time moments $t = n\tau$. The system parameters and the number of cars are specified so that the virtual car ensemble imitate the real characteristics of traffic flow, at least semiquantitatively. The lower fragment in Fig. 3 exhibits the net value of the identification errors, $A + B$, vs. the acceleration threshold a_{\max} . As could be expected, the present results demonstrate the fact that the car identification algorithm attains its maximal efficiency when

$$a_{\max} = \frac{4(\xi_{1M} + \xi_{2M})}{\tau^2}, \quad (3)$$

and, in particular, for $\xi_{1M} = 0.5$ m and $\xi_2 = 1.5$ m the optimal acceleration threshold is about $a_{\max} \sim 50$ m/s².

Second, the developed algorithm has been verified using the available airborne traffic data collected during Soccer Championship 2006 in Stuttgart within the DLR project ‘‘Soccer’’ [3]. These data undergone manual processing, so initially we had a collection of vehicle trajectories regarded as real keeping in mind the human abilities. The vehicle identification algorithm has given the result depicted in Fig. 4. For

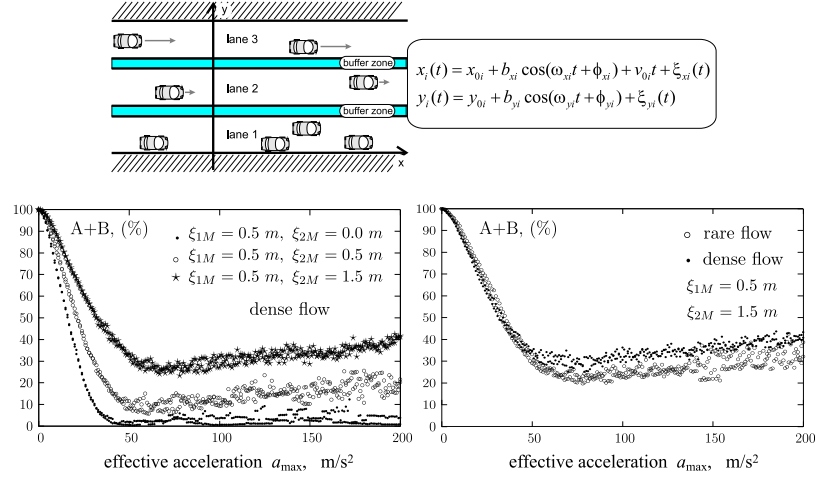


Fig. 3. Airborne data simulator, “Virtual Road”, used to verify the vehicle identification algorithm (upper fragment) and the corresponding results of the car identification routine (lower fragment). The subscript M at the noise components ξ_{iM} stands for their amplitudes.

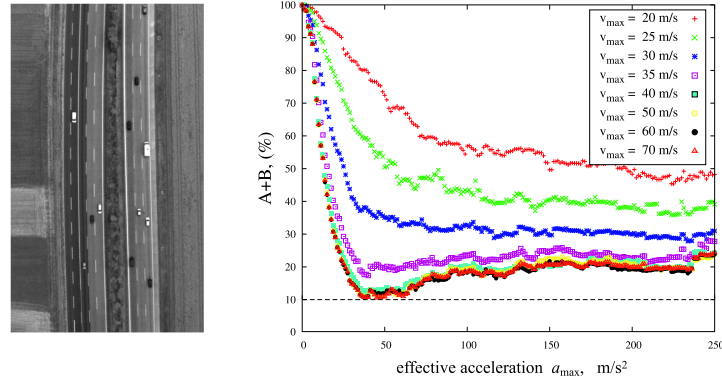


Fig. 4. The airborne data collected during the Soccer Championship 2006 in Stuttgart. Typical example of the analyzed video data (left fragment) and the results of car identification routine vs. the acceleration threshold (right fragment).

these data, again, the optimal value of the acceleration threshold meets relation (3). Figure 4 presents also the efficiency of the car identification algorithm for different values of the velocity threshold v_{\max} . As seen the imposition of the additional speed limitation constraint reduces the algorithm efficiency. In other words, constraints (1) interfere with each other and, thus, should be used separately. As should be expected the measurement errors and the optimal acceleration threshold are again related by expression (3).

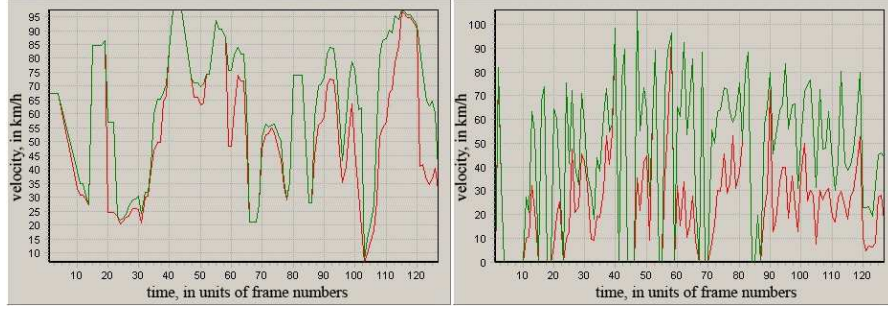


Fig. 5. Time-mean speed (green) and space-mean speed (red) reconstructed using the smoothed vehicle trajectories (left fragment) and the same data obtained using the neighboring points directly. The airborne data of pilot flights in Berlin, 2004, the LUMOS project.

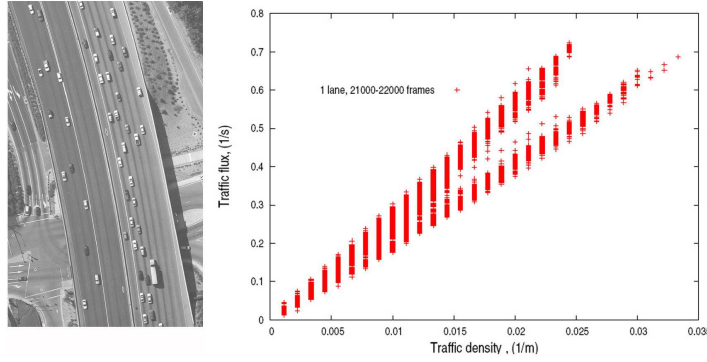


Fig. 6. Fundamental diagram (right fragment) and an example of the analyzed video data (left fragment). The NGSIM “First Prototype” dataset [4].

Mean Velocity of Traffic Flow and Fundamental Diagram

Because of the considerable errors in the vehicle coordinates the found successive positions of a car cannot be used directly to calculate its velocity. However, the reconstructed trajectories enable one to overcome this problem by fitting a rather smooth trajectory to the found data. In this way we have analyzed the empirical data collected during pilot flights of an airplane in Berlin, 2004 (DLR, LUMOS project). The mean velocity of traffic flow was calculated, first, by smoothing the reconstructed vehicle trajectories via the Savitzky-Golay filter and, then, averaging the velocities over the observed car ensemble. The results are illustrated in Fig. 5. As seen the time pattern of traffic flow speed obtained by smoothing the reconstructed vehicle trajectories gives much more adequate description of traffic flow.

Using the developed technique we have analyzed also the NGSIM “First Prototype” dataset consisting of vehicle trajectories on a half-mile section of Interstate 80 in Emeryville, California, for one half of hour [4]. The system portrait on the phase plane “traffic flow rate – car density” was drawn using the mean car velocity calculated via the developed technique and car density obtained by just counting the detected objects (Fig. 6). No widely scattered states are visible, instead, branching is fixed. This result again poses the question about the necessity to single out the vehicle flow discreteness in analyzing the states of traffic flow [5]. It should be noted that the developed approach depresses this discreteness effect.

Conclusion

We have developed the three-frame-algorithm of reconstructing vehicle trajectories from airborne traffic data, which evaluates the proximity of objects in the neighboring frames in terms of acceleration. The acceleration threshold a_{\max} is determined by the car measurement accuracy. Using the “Virtual Road” simulator and the dataset collected within the project “Soccer” (DLR, Stuttgart, 2006) the value of $a_{\max} \sim 40\text{--}50 \text{ m/s}^2$ is found and the possibility of decreasing the identification error down to 5–30 % is shown.

Using one of the NGSIM datasets it has been demonstrated that for the observed congested traffic the fundamental diagram splits into two branches when the car density exceeds some value rather than exhibits the widely scattered states. This result again poses a question whether the discreteness of traffic flow could be responsible for the appearance of widely scattered states on the fundamental diagrams. Naturally, the unambiguous answer requires special and detailed investigation.

Acknowledgement. This work was supported in part by INTAS project 04-78-7185, DFG project MA 1508/8-1, and RFBR grants 06-01-04005, 05-01-00723, and 05-07-90248.

References

1. I. Ernst, S. Sujew, K.-U. Thiessenhusen, M. Hetscher, S. Raßmann and M. Ruhé: *LUMOS - Airborne Traffic Monitoring System*. In: Proceedings of the IEEE 6th International Conference On Intelligent Transportation Systems; Shanghai (China), 2003 (CD-ROM).
2. H. Hetzheim, A. Börner: *Vehicle detection from airborne images by seperating of texture properties and their fusion*. In: Image and Vision Computing, New Zealand, 2003, Proceedings pp. 48–53, (Palmerston North, 2003).
3. Martin Ruhé, Reinhart Kühne, Ines Ernst, Sergey Zuev, and Eileen Hipp, *Air borne systems and datafusion for traffic surveillance and forecast for the soccer world cup*. In: Proceedings of 86-th Annual Meeting Transportation Research Board, January, 2007, Washington, D.C.
4. Next Generation Simulation Community, <http://ngsim.camsys.com>.
5. I. Lubashevsky, R. Mahnke, P. Wagner, and S. Kalenkov, Phys. Rev. E **66**, 016117 (2002).